

Accepted Manuscript

Synthesis and biological evaluation of isoindoloisoquinolinone, pyroloisoquinolinone and benzoquinazolinone derivatives as PolyADP-Ribose Polymerase-1 inhibitors

Arumugam Suyavaran, Chitteti Ramamurthy, Ramachandran Mareeswaran, Yagna Viswa Shanthi, Jayaraman Selvakumar, Selvaraj Mangalaraj, Muthuvel Suresh Kumar, Chinnasamy Ramaraj Ramanathan, Chinnasamy Thirunavukkarasu

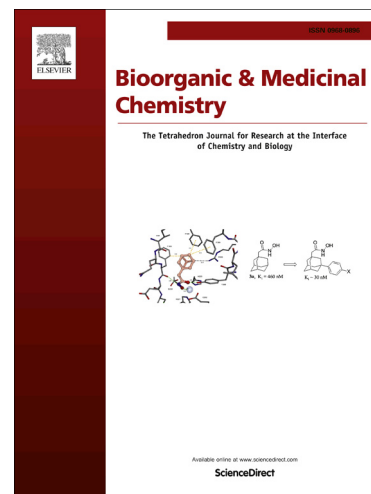
PII: S0968-0896(14)00865-7
DOI: <http://dx.doi.org/10.1016/j.bmc.2014.12.017>
Reference: BMC 11949

To appear in: *Bioorganic & Medicinal Chemistry*

Received Date: 1 October 2014
Revised Date: 24 November 2014
Accepted Date: 11 December 2014

Please cite this article as: Suyavaran, A., Ramamurthy, C., Mareeswaran, R., Viswa Shanthi, Y., Selvakumar, J., Mangalaraj, S., Suresh Kumar, M., Ramaraj Ramanathan, C., Thirunavukkarasu, C., Synthesis and biological evaluation of isoindoloisoquinolinone, pyroloisoquinolinone and benzoquinazolinone derivatives as PolyADP-Ribose Polymerase-1 inhibitors, *Bioorganic & Medicinal Chemistry* (2014), doi: <http://dx.doi.org/10.1016/j.bmc.2014.12.017>

This is a PDF file of an unedited manuscript that has been accepted for publication. As a service to our customers we are providing this early version of the manuscript. The manuscript will undergo copyediting, typesetting, and review of the resulting proof before it is published in its final form. Please note that during the production process errors may be discovered which could affect the content, and all legal disclaimers that apply to the journal pertain.



**Synthesis and biological evaluation of isoindoloisoquinolinone, pyroloisoquinolinone
and benzoquinazolinone derivatives as PolyADP-Ribose Polymerase-1 inhibitors**

Arumugam Suyavaran^a, Chitteti Ramamurthy^a, Ramachandran Mareeswaran^a, Yagna Viswa
Shanthi^a, Jayaraman Selvakumar^b, Selvaraj Mangalaraj^b, Muthuvel Suresh Kumar^c,
Chinnasamy Ramaraj Ramanathan^{b*} and Chinnasamy Thirunavukkarasu^{a*}

^aDepartment of Biochemistry and Molecular Biology, Pondicherry University, Puducherry
605 014, India. ^bDepartment of Chemistry, Pondicherry University, Puducherry 605 014,
India. ^cCentre for advance studies in Bioinformatics, School of Life Sciences, Pondicherry
University, Puducherry- 605 014

* Corresponding authors: Tel.:+91 413 2654872; Fax: +91 413 2655255; E-mail address:
tchinnasamy@hotmail.com (C. Thirunavukkarasu); Tel.: +91 413 2654416; Fax: +91-413
2656740; Email: crrnath.che@pondiuni.edu.in (C. R. Ramanathan).

Abstract

A series of novel fused isoquinolinones with isoindoloisoquinolinone, pyroloisoquinolinone, and benzoquinazolinone skeletons were synthesized from corresponding phenethylimides. The isoquinolinone derivatives were evaluated for their protective effect on chicken erythrocytes subjected to oxidative damage. The effect of isoquinolinone derivatives were analysed by estimation of cell viability, antioxidant enzyme activities, DNA damage (comet assay), PARP-1 inhibition assay and molecular docking of the compounds with PARP-1 active site. The compounds **CRR-271**, **CRR-288** and **CRR-224+225** showed significant protective effect at 100 μ M concentration. The PARP-1 inhibition assay revealed the IC₅₀ values of **CRR-271**, **CRR-288** and **CRR-224+225** as <200 nM, further molecular docking studies shows higher binding energies with PARP-1 active site. Interesting findings in this study suggest that the novel isoquinolinone derivatives inhibit PARP-1 activity and protect cells against oxidative DNA damage, which could be implemented in the treatment of inflammatory diseases.

Keywords:

Isoquinolinones; Inflammation; DNA damage; Oxidative stress; PARP-1

1. Introduction

Cellular oxidative stress is one of the major causative in the development of degenerative diseases. It results due to the imbalance between antioxidants and free radicals, predominantly reactive oxygen species (ROS) within the cell.¹ The ROS mainly comprise of superoxide anions, hydroxyl radicals (OH^\bullet) and hydrogen peroxide (H_2O_2). ROS interact with all cellular macromolecules at various levels and impair their function which is the mainstay for initiation and progression of several degenerative disorders.^{1,2} Among the ROS, H_2O_2 is the most stable, freely diffusible and serves as the source for OH^\bullet , hence it contributes more to the oxidative insult than the rest of ROS. The oxidative stress in cells is usually augmented by inflammatory mediators such as interleukins and cytokines leading to different forms of cell death.^{1,3}

Sustained oxidative stress in chronic inflammatory conditions would eventually lead to necrosis, which is an uncontrolled and passive process of cellular degeneration resulting from depletion of ATP content of a cell.^{4,5} Damaged cells, further recruit the inflammatory cells, by releasing the various pro-inflammatory mediators into the surrounding tissues, which worsen the tissue injury.³ Several molecular mediators have been identified as culprit for initiation and progression of cell degeneration during necrosis. Poly (ADP-ribose) polymerases-1 (PARP-1) is one such molecule which has recently gained importance as a key initiator for necrosis activated by oxidative stress.⁶

PARP-1 also known as NAD^+ , ADP-ribosyltransferase-1 or poly[ADP-ribose] synthase-1, is a chromatin-associated, highly conserved enzyme with molecular weight of 116 kDa.⁷ It gets activated in response to DNA damage, which is initiated due to imbalance in oxidative stress. The activated PARP-1 binds to damaged DNA and initiates the synthesis of long branches of poly (ADP-ribose) polymers (PAR chains) using NAD^+ .⁸ In most severe

and sustained oxidative stress and inflammatory conditions, excessive DNA damage triggers the hyper activation of PARP-1 and it leads to the depletion of NAD^+ . Depleted NAD^+ eventually leads to exhaustion of ATP reserve of the cell, which results in necrotic cell death. Inhibition of hyper activated PARP-1 would lead to reduced consumption of NAD^+ and restoration of ATP reserve which in turn prevents the cell death. Hence, PARP-1 inhibitors are recently gaining more attention as novel therapeutic agents in the treatment of inflammatory diseases.⁹⁻¹¹

Extensive investigations have been conducted in the identification of novel PARP-1 inhibitors. Various approaches to design the scaffolds for PARP-1 inhibitors based on the prototypical PARP-1 inhibitor benzamide as pharmacophore, which mimics the nicotinamide moiety of NAD^+ .¹²⁻¹⁴ Five PARP-1 inhibitors are currently under the clinical oncology trials (AG014699, KU59436, BSI-201, INO-1001 and GPI 21016).^{15,16} According to the structure-activity relationship studies several molecules with benzamide backbone are enriching the potent inhibitor for PARP-1 (Fig. 1).

[insert Figure 1]

Fused isoquinolinones are heterocyclic motifs that are formed by the fusion of benzene ring with isoindolone or pyrrolone or piperidone units. The derivatives of isoquinolinones show diverse biological activities like inhibition of PARP-1,¹⁷⁻¹⁹ anti-inflammatory activity,²⁰ anti-cancer,²¹ and vaso relaxation²². The wide applicability of isoquinolinone units against various biological targets prompted us to investigate PARP-1 inhibitory activity of the fused isoquinolinone derivatives. The isoquinolinone derivatives used in this study are analogues of pharmacologically available alkaloids such as nuevamine and crispine-A.²³⁻²⁵

In vitro exposure of cells to H₂O₂ for a short period has shown to implicate DNA damage to the cells. Prolonged exposure to H₂O₂ has shown to induce irreversible damage to the cellular DNA.²⁶⁻²⁸ Hence this *in vitro* model is considered to mimic cellular pathology during oxidative stress. In the present study, we evaluated the ameliorative effect of 11 different isoquinolinone derivatives against H₂O₂ induced oxidative DNA damage in chick red blood cells (RBCs).

2. Results and Discussion

The PARP-1 activity is increased during inflammatory conditions and leads to depletion of energy reserves of the cell which results in cell death. Many novel isoquinolinones have been discovered with anti-inflammatory activity and are gaining importance due to their potent PARP-1 inhibitory activity.^{17,18} This is the due reason for isoquinolinones to gain more attention over existing non-steroidal anti-inflammatory drugs. Since inflammatory pathway is activated in various diseases, isoquinolinones would gain importance in future as multi-therapeutic compound. Hence, it is essential that the interaction of isoquinolinones at cellular and molecular level to be tested extensively.

Unlike regular eukaryotic nucleus, the chicken erythrocytes lack a intricate nucleoprotein complex, making it a simpler system for investigation of drug interaction at nuclear level.²⁹ Moreover, the chicken erythrocytes contain active mitochondria which significantly contribute to internal ROS generation.³⁰ Hence in the current study we analyzed the protective ability of the chosen isoquinolinone derivatives namely **CRR-222, CRR-203, CRR-211, CRR-271, CRR-204, CRR-228, CRR-227, CRR-213, CRR-238, CRR-267** and **CRR-224+225** (Fig. 1) against H₂O₂ induced oxidative damage in RBCs. H₂O₂ induced cellular toxicity is a standard model to assess the protective effects of pharmacophores against oxidative stress induced damage.³¹⁻³³ Previous studies show that chick RBCs exposed

to oxidative damage is a suitable model for assessment of antioxidant status upon treatment of pharmacophores.³³⁻³⁵

2.1. Synthesis of isoquinolinone derivatives

The isoquinolinone derivatives used in this study (isoindoloisoquinolinone, pyroloisoquinolinone and benzoquinalizinone skeletons) were synthesized from corresponding phenethylimides *via* electrophilic activation of imide carbonyl group by trifluoromethanesulfonic acid (TfOH).³⁶ Phenethylimides undergo intramolecular 6-*exo-trig* cyclization with electrophilically activated imide carbonyl group (by TfOH) and generate fused cyclic *N*-acyliminium ion. This *N*-acyliminium ion on treatment with oxygen nucleophile (H₂O) delivers fused hydroxy-isoquinolinones or with hydride nucleophile (NaBH₄) delivers fused isoquinolinones (Fig. 2).

[insert Figure 2]

The rigid bicyclic isoquinolinone **CRR-267** synthesis starts from the preparation of corresponding imide by condensation of 3,4-dimethoxy phenethylamine **11** and anhydride **12**. The anhydride **12** is in turn derived from anthracene and maleic anhydride through Diels-Alder reaction. The imide **13** under established cyclization condition delivers the rigid isoquinolinone **CRR-267** in 87% yield (Fig. 3). The crystal structure of **CRR-267** was obtained and has been represented in Figure 4.

[insert Figure 3]

[insert Figure 4]

The molecules **CRR-203**, **CRR-222**, **CRR-211**, **CRR-271**, **CRR-204**, **CRR-228** and **CRR-227** are composed of the essential PARP-1 inhibitory benzamide core fused with isoquinoline

skeleton as well as hydroxyl group. The molecules such as **CRR-224** and **CRR-225** contain two methoxy substitutions in benzamide core. The molecules **CRR-213**, **CRR-238** and **CRR-267** possess benzylamide unit instead of benzamide in addition to a rigid bicyclic unit. The presence of these structural features prompted us to examine these benzamide fused molecules for their activity against PARP-1. The regioisomeric mixtures **CRR-224** and **CRR-225** were obtained in 1:1 ratio following the established cyclization procedure.

2.2. Acridine orange (AO) and Ethidium bromide (EB) staining

AO and EB staining method is superior over other staining methods for detection of cell viability upon oxidative damage.³⁷ The viability of RBCs after exposure to 100 μM H_2O_2 for 1 hour at 37 $^\circ\text{C}$, was assessed by AO and EB staining. The untreated RBCs and the RBCs exposed to 0.5% DMSO alone showed viability of about 94%, while the viability of RBCs exposed to H_2O_2 alone was reduced to 41%. We have not observed any change in normal RBCs viability when pre-treated with various concentrations of different fused isoquinolinone derivatives (25 μM to 100 μM – data not shown). The RBCs were pre-treated with various concentrations (25 μM to 100 μM) of different fused isoquinolinone derivatives for 1 hour at 37 $^\circ\text{C}$ and then challenged against 100 μM H_2O_2 for 1 hour at 37 $^\circ\text{C}$. We have observed increased viability of cells pre-treated with all the compounds, which was also dose dependent. Interestingly the compounds **CRR-271** and **CRR-224+225** at the concentrations of 100 μM (Other concentration data's are not shown) showed viability of <90% (Table 1; Fig. 5). Other compounds show moderate cell viability ranging from 75 – 87% and the least (54%) viability was observed for **CRR-204** (Table 1). Previous studies have also reported the oxidative DNA damage by employing AO and EB staining method and have shown similar results for other pharmacophores.³⁸⁻³⁹

[insert Table 1]

[insert Figure 5]

2.3. Antioxidants and Lipid peroxidation

In the current study, a significant decrease ($P \leq 0.05$) in the activities of catalase and superoxide dismutase (SOD) was found in the RBCs treated with 100 μM H_2O_2 alone, when compared to untreated RBCs. Pre-treatment of isoquinolinone derivatives demonstrated restoration of the antioxidant enzyme activities. RBCs pre-treated with **CRR-271**, **CRR-267** and **CRR-224+225** at the concentration of 100 μM showed significant protection ($P \leq 0.05$) in the superoxide dismutase and catalase activities when compared to RBCs treated with H_2O_2 alone (Table 2).

[insert Table 2]

A significant increase ($P \leq 0.05$) in the extent of lipid peroxidation was observed in the H_2O_2 alone treated RBCs when compared to the untreated RBCs (Table 2). The RBCs pre-treated with **CRR-271**, **CRR-228**, **CRR-267** and **CRR-224+225** at the concentration of 100 μM showed significant decrease in lipid peroxidation level when compared to RBCs treated with H_2O_2 alone ($P \leq 0.05$). Other isoquinolinone derivatives did not show such restoration in above enzyme activities and lowering of lipid peroxidation level. Vehicle control showed the values similar to that of normal control in all assays. Previous works have shown that H_2O_2 induced damage to the membrane via lipid peroxidation can be suppressed by protective effect of the pharmacophores with antioxidant properties.⁴⁰ Lipid peroxidation is the one of the main reasons for aggravation of oxidative damage, since it leads to a chain reaction producing lipid peroxy radicals, which ultimately results in altered membrane function and leakage of cellular contents leading to further inflammatory progression.⁴¹⁻⁴²

2.5. Isoquinolinone on genomic DNA damage

Single cell alkaline gel electrophoresis (Comet assay) in normal and DMSO treated RBCs demonstrated comet pattern with higher percent of DNA in head region (>95%). RBCs treated with H₂O₂ alone produced comet with about 45% of DNA in tail depicting damage to the genomic DNA. Pre-treatment of cells with 100 µM concentration of **CRR-222**, **CRR-271**, **CRR-228** and **CRR-224+225** showed comet with >90% DNA in head region (Table 3). **CRR-211**, **CRR-204** and **CRR-213** showed negligible effect on DNA protection ($P \leq 0.05$). Similar reports with comet assay on DNA damage and study of protective effects of antioxidants at nuclear level have been reported earlier.⁴³⁻⁴⁵

[insert Table 3]

2.6. PARP-1 inhibition assay

The potential of PARP-1 inhibitory activity of **CRR-271**, **CRR-228** and **CRR-224+225** were evident from the PARP-1 enzyme inhibition assay. **CRR-228** and **CRR-224+225** have IC₅₀ values of 138.5 nM and 186.5 nM respectively, while the IC₅₀ value of **CRR-271** is 216.2 nM. Thus the IC₅₀ values of these compounds are comparable to that of the standard isoquinolinone, such as 3,4-dihydro-5-[4-(1-piperidinyloxy)butoxy]-1(2H)-isoquinolinone (DPQ) whose IC₅₀ is 53.6 nM. The IC₅₀ value of **CRR-238** is <500 nM while the other isoquinolinone compound used in this study have IC₅₀ values >800 nM making them less suitable candidates as potent PARP-1 inhibitor. Though IC₅₀ values of these compounds are in nM concentrations, on the other hand µM concentrations (shows positive effect in the present study) are necessary to counteract the oxidants such as H₂O₂ and to gain access into cellular milieu and bind with active PARP-1 enzyme. Sakaue *et al* have reported

antioxidant activity of isoquinolinones in their study, where they have used 30 μM concentration of DPQ (IC_{50} -53.5 nM) for co-treatment of rat cerebellar granule cells with methyl mercury.⁴⁶

2.7. Interaction of isoquinolinone derivatives with active site of PARP-1

The docking studies revealed that **CRR-271**, **CRR-228** and **CRR-224+225** are the isoquinolinones which form hydrogen bonds with the active site amino acids such Gly 863, Lys 903, Tyr 907 and Tyr 896 and have binding energy >-7.3 kcal/mol (Table. 4). **CRR-271** forms three hydrogen bonds, each with Lys 903, Tyr 907 and Tyr 896 respectively with a binding energy of -7.88 kcal/mol (Table.4). **CRR-228** and **CRR-224+225** form hydrogen bond with Tyr 896 and Gly 863 respectively with binding energy of -7.33 kcal/mol and -8.43 kcal/mol. **CRR-267** has binding energy more >-8.00 kcal/mol, however it does not form any hydrogen bonds with any of the amino acids in the active site, further it has an IC_{50} value of >800 nM hence it may not be a suitable competitive inhibitor of PARP-1, though its inhibition might be through some other mode. On the other hand **CRR-271**, **CRR-228** and **CRR-224+225** have reasonable binding energy, forms hydrogen bonds with active site amino acids and these compounds have IC_{50} values 138.5 nM – 216.2 nM, hence we suggest that **CRR-271**, **CRR-228** and **CRR-224+225** may serve as potent PARP-1 inhibitor.

The binding score of DPQ – a standard isoquinolinone was found to be -8.67 , which is comparable to the binding scores of the above compounds. The docking results correlate well with other biochemical results, suggesting the potency of these compounds to function as antioxidants and PARP-1 inhibitors. Moreover, the anti-inflammatory property of indole and pyrrole derivatives gives an added advantage to the isoquinolinones to act synergistically and efficiently by preventing inflammatory degeneration of the cells in addition to blocking PARP-1 as required in the treatment of several chronic inflammatory disease.^{47,48} Hence even

though the docking scores of isoquinolinones under study are lower than (but comparable to) the DPQ, they are better candidates for clinical consideration because of their additional anti-oxidant property.

[insert Table 4]

3. Conclusion

Present study concludes that the tetrahydroisoquinolinone derivatives **CRR-271**, **CRR-228** and **CRR-224+225** which are novel derivatives of isoquinolinone, protect chick RBCs against H₂O₂ induced damage at 100 µM concentration as evident from the cell viability, antioxidant enzyme activities and lipid peroxidation at cellular and genomic DNA damage protection at nuclear level. The potential inhibitory activity of **CRR-271**, **CRR-228** and **CRR-224+225** is evident from PARP-1 inhibition assay. The docking studies show that **CRR-271**, **CRR-228** and **CRR-224+225** form hydrogen bonds with active site amino acids suggesting competitive binding with PARP-1 substrate binding site. Further studies are necessary to establish the molecular interactions and pharmacodynamics of these novel isoquinolinone derivatives, which would see them as effective synergistic combinations along with existing anti-inflammatory drugs.

4. Experimental Section

4.1. General

We performed Column chromatography on MerckTM silica gel 100-200 mesh. TLC (Thin layer chromatography) analyses were facilitated using phosphomolybdic acid stain and permanganate stain and visualized under UV light with Merck 60 F₂₅₄ pre-coated silica

plates. Melting points reported here are uncorrected and were determined using EZ Melt, Stanford Research Systems, USA. Infrared spectra were recorded on Thermo Nicolet 6700 FT-IR (Fourier transform infra-red) Spectrophotometer using KBr thin films, and are reported in frequency of absorption (cm^{-1}). Mass spectra, GC-MS (Gas chromatography – mass spectrometry), were recorded on Varian GC-MS (CP-3800/Saturn 2200). LDI-MS (Laser desorption ionization – mass spectrometry) were recorded on ABI Voyager DE-STR mass spectrometer. HRMS (High resolution mass spectrometry) were measured with micro mass Q-TOF (ESI-HRMS). ^1H and ^{13}C NMR were recorded on Bruker AVANCE 400 spectrometer. All the NMR (Nuclear magnetic resonance) spectra were recorded at room temperature in CDCl_3 or $\text{DMSO}-d_6$ using TMS (Tetramethylsilane) as an internal standard. The chemical shifts are expressed in δ ppm down field from the signal of internal TMS. Coupling constant (J) values are given in Hz. The splittings in spectra are reported as: s = singlet, d = doublet, t = triplet, q = quartet, qn = quintet, m = multiplet, dd = doublet of doublet, ddd = doublet of doublet of doublets, dt = doublet of triplet, td = triplet of doublet, br s = broad singlet. All the anhydrides are used as purchased. By following our earlier reported procedure we have synthesized all the isoquinolinone molecules.³⁶

4.2. Typical procedure to synthesize of isoquinolinone molecules

An oven dried two neck round bottom flask bearing septum in side arm was cooled to room temperature under a steady stream of nitrogen gas flow. The flask was charged with stirring bar, imide (0.5 mmol, 1 equiv) and dry dichloromethane (5 mL) and cooled down to 0 °C (using ice). To this solution TfOH (0.2 mL, 4 equiv.) was added with stirring. After completion of reaction (monitored by TLC), the reaction mixture was quenched with water (10 mL) followed by NaHCO_3 (1g). The organic layer was separated and aqueous layer was extracted with dichloromethane (2 x 15 mL). The combined organic extract was washed with

brine solution and dried over anhydrous Na₂SO₄. The extract was filtered and the solvent was removed under vacuum to dryness on rotary evaporator which yielded the crude cyclized product. The dried compound was purified through the short silica gel column chromatography using ethyl acetate and hexane (50:50) as eluent.

4.2.1. 12b-Hydroxy-2,3-dimethoxy-5,12b-dihydro-6H-isoindolo[1,2-a]isoquinolin-8-one

(CRR-203): Following the general procedure, *N*-[2-(3,4-dimethoxy-phenyl)ethyl]-phthalimide furnished the cyclized product as colorless solid, 149 mg (96% yield), Mp 159 °C, IR (KBr, cm⁻¹): 3331, 1672, 1614, 1518. ¹H NMR (400 MHz, CDCl₃): δ 7.99 (d, *J* = 7.6 Hz, 1H), 7.67 (d, *J* = 7.6 Hz, 1H), 7.63 (td, *J* = 7.6, 1.2 Hz, 1H), 7.47 (td, *J* = 7.6, 1.2 Hz, 1H), 7.41 (s, 1H), 6.56 (s, 1H), 4.16 (ddd, *J* = 13.2, 7.6, 1.6 Hz, 1H), 4.04 (s, 1H), 3.95 (s, 3H), 3.83 (s, 3H), 3.42-3.35 (m, 1H), 2.95-2.87 (m, 1H), 2.67 (ddd, *J* = 16.0, 8.0, 1.6 Hz, 1H). ¹³C NMR (100 MHz, CDCl₃): δ 167.4, 149.4, 148.2, 148.0, 132.7, 130.6, 129.5, 127.8, 127.6, 123.7, 123.0, 111.5, 110.4, 86.4, 56.2, 56.0, 34.9, 29.1. LDI-MS (*m/z*); Found 312.1248 and calculated 312.1236 for C₁₈H₁₇NO₄⁺[M+H].

4.2.2. 12b-Hydroxy-3-methoxy-5,12b-dihydro-6H-isoindolo[1,2-a]isoquinolin-8-one

(CRR-204): Following the general procedure, *N*-[2-(3-methoxy-phenyl)ethyl]-phthalimide furnished the cyclized product as colorless solid, 130 mg (93% yield), Mp 169 °C. IR (KBr, cm⁻¹): 3265, 1681, 1613, 1580, 1407. ¹H NMR (400 MHz, DMSO-*d*₆): δ 8.12 (d, *J* = 8.0 Hz, 1H), 7.89 (d, *J* = 4.8 Hz, 1H), 7.63-7.68 (m, 2H), 7.51 (td, *J* = 7.6, 0.8 Hz, 1H), 6.89 (s, 1H), 6.84 (dd, *J* = 8.4, 2.4 Hz, 1H), 6.72 (d, *J* = 2.4 Hz, 1H), 4.23-4.17 (m, 1H), 3.71 (s, 3H), 3.45-3.38 (m, 1H), 2.79 (dd, *J* = 7.6, 4.0 Hz, 2H). ¹³C NMR(100 MHz, DMSO-*d*₆): δ 165.8, 158.5, 148.7, 135.9, 132.2, 130.2, 129.6, 129.2, 129.1, 123.7, 122.3, 113.0, 112.9, 85.4, 55.0, 29.0, 34.1. LDI-MS (*m/z*) Found 282.1112 and calculated 282.1130 for C₁₇H₁₅NO₃⁺ [M+H].

4.2.3. 12b-Hydroxy-3,4-dimethoxy-5,12b-dihydro-6H-isoindolo[1,2-a]isoquinolin-8 one

(CRR-211): Following the general procedure, *N*-[2-(2,3-dimethoxy-phenyl)ethyl]-phthalimide furnished the cyclized product as colorless solid, 132 mg (85% yield), Mp 198 °C. IR (KBr, cm^{-1}): 3293, 1678, 1602, 1458. ^1H NMR (400 MHz, CDCl_3): δ 7.99 (d, $J = 8.0$ Hz, 1H), 7.69 (s, 1H), 7.69-7.68 (m, 1H), 7.62 (td, $J = 7.6, 1.2$ Hz, 1H), 7.46 (td, $J = 7.2, 0.8$ Hz, 1H), 6.87 (d, $J = 8.8$ Hz, 1H), 4.20 (ddd, $J = 13.2, 6.4, 2.4$ Hz, 1H), 3.83 (s, 3H), 3.81 (s, 1H), 3.73 (s, 3H), 3.41-3.34 (m, 1H), 3.02 (ddd, $J = 16.8, 4.4, 2.0$ Hz, 1H), 2.81–2.72 (m, 1H). ^{13}C NMR (100 MHz, CDCl_3): δ 167.1, 152.4, 147.9, 146.2, 132.5, 130.5, 129.6, 129.5, 128.9, 123.5, 123.4, 123.2, 110.8, 86.1, 60.1, 55.7, 34.2, 23.4. LDI-MS (m/z) Found 312.1257 and Calculated 312.1236 for $\text{C}_{18}\text{H}_{17}\text{NO}_4^+[\text{M}+\text{H}]$.

4.2.4. 8,10-Dimethoxy-1,2,5,6-tetrahydropyrrolo[2,1-a]isoquinolin-3(10bH)-one (CRR-213):

Cyclization using TfOH followed by reduction using $\text{NaBH}_4/\text{MeOH}$, *N*-[2-(3,5-dimethoxyphenyl)-ethyl]succinimide furnished the cyclized product **CRR-213** as colorless solid, 109 mg (87% yield), Mp 121-122 °C. IR (KBr, cm^{-1}): 2974, 1689, 1586, 1442. ^1H NMR (400 MHz, CDCl_3): δ 6.33 (d, $J = 2.4$ Hz, 1H), 6.24 (d, $J = 2.4$ Hz, 1H), 4.75-4.71 (m, 1H), 4.40-4.35 (m, 1H), 3.79 (s, 3H), 3.77 (s, 3H), 2.87-2.78 (m, 3H), 2.66-2.62 (m, 1H), 2.53-2.47 (m, 1H), 2.40-2.33 (m, 1H), 1.69-1.60 (m, 1H). ^{13}C NMR (100 MHz, CDCl_3): δ 173.4, 159.2, 157.7, 135.8, 118.6, 104.6, 96.9, 55.3, 55.2, 54.9, 36.6, 31.6, 29.7, 28.1. LDI-MS (m/z) Found 248.1300 and calculated 248.1287 for $\text{C}_{14}\text{H}_{17}\text{NO}_3^+[\text{M}+\text{H}]$.

4.2.5. 12b-Hydroxy-1,4-dimethoxy-5,12b-dihydro-6H-isoindolo[1,2-a]isoquinolin-8-one

(CRR-222): Following the general procedure, *N*-[2-(2,5-dimethoxy-phenyl)ethyl]-phthalimide furnished the cyclized product as colorless solid, 135 mg (87% yield), Mp 165-166 °C. IR (KBr, cm^{-1}): 3398, 3054, 2925, 2854, 1717, 1675, 1586, 1458, 1290, 1063, 1020, 887, 739. ^1H NMR (400 MHz, CDCl_3): δ 8.16-8.14 (m, 1H), 7.79-7.77 (m, 1H), 7.51 (td, $J = 7.5, 1.3$ Hz, 1H), 7.45 (td, $J = 7.5, 1.0$ Hz, 1H), 6.84 (d, $J = 8.9$ Hz, 1H), 6.76 (d, $J = 8.9$ Hz,

1H), 4.53 (ddd, $J = 13.0, 5.8, 1.0$ Hz, 1H), 4.45 (s, 1H), 4.07 (s, 3H), 3.75 (s, 3H), 3.30 (td, $J = 13.0, 3.5$ Hz, 1H), 2.91 (ddd, $J = 17.2, 3.5, 1.0$ Hz, 1H), 2.68-2.59 (m, 1H). ^{13}C NMR (100 MHz, CDCl_3): δ 167.8, 151.7, 151.2, 148.8, 132.4, 130.8, 129.4, 126.7, 125.6, 124.1, 123.2, 110.1, 108.9, 87.1, 55.8, 55.5, 34.7, 24.1. HRMS-ESI (m/z) found 334.1053 and calculated 334.1055 for $\text{C}_{18}\text{H}_{17}\text{NO}_4$ [M+Na].

4.2.6. 10,11-Dimethoxy-5,11b-dihydro-6H-1,3-dioxo-6a-aza-indeno[5,6-c]fluoren-7-one and 8,9-Dimethoxy-5,11b-dihydro-6H-1,3-dioxo-6a-aza-indeno[5,6-c]fluoren-7-one

(CRR-224+CRR-225): Cyclisation using TfOH and reduction using NaBH_4 / TFA, 2-[2-(1,3-benzodioxol-5-yl)ethyl]-4,5-dimethoxy-1H-isoindole-1,3(2H)-dione furnished the cyclized product as colorless solid, 145 mg (86% yield), IR (KBr, cm^{-1}): 2972, 2940, 2841, 1681, 1620, 1446, 1408, 1273, 1220, 1035; ^1H NMR (400 MHz, CDCl_3): δ 7.58 (d, $J = 8.0$ Hz, 1H), 7.43 (dd, $J = 0.8, 8.4$ Hz, 1H), 7.32 (s, 1H), 7.14 (d, $J = 8.0$ Hz, 1H), 7.07 (d, $J = 8.4$, 1H), 7.03 (s, 1H), 6.66 (s, 1H), 6.65 (s, 1H), 5.95 (d, $J = 1.2$ Hz, 1H), 5.92 (d, $J = 1.2$ Hz, 1H), 5.89 (d, $J = 1.2$ Hz, 1H), 5.86 (d, $J = 1.2$ Hz, 1H), 5.63 (s, 1H), 5.45 (s, 1H), 4.34-4.28 (m, 1H), 4.07 (s, 3H), 4.0-4.09 (m, 1H), 3.99 (s, 3H), 3.97 (s, 3H), 3.90 (s, 3H), 3.59-3.53 (m, 1H), 3.42-3.36 (m, 1H), 3.05-2.94 (m, 2H), 2.90-2.82 (m, 1H), 2.79-2.75 (m, 1H). ^{13}C NMR (100 MHz, CDCl_3): δ 167.6, 166.2, 155.5, 152.8, 146.7, 146.5, 146.4, 144.3, 137.6, 136.1, 128.8, 128.4, 128.3, 127.8, 126.6, 125.1, 119.7, 118.4, 116.2, 113.2, 109.0, 108.4, 107.5, 105.5, 101.1, 100.9, 62.5, 60.5, 58.4, 58.0, 56.7, 56.3, 38.8, 38.3, 29.3, 28.9.

4.2.7. 12b-Hydroxy-3-methyl-5,12b-dihydro-6H-isoindolo[1,2-a]isoquinolin-8-one

(CRR-227): Following the general procedure, *N*-[2-(3-methyl-phenyl)ethyl]-phthalimide, furnished the cyclized product as colorless solid, 103 mg (78% yield), Mp 174-175 °C. IR (KBr, cm^{-1}): 3269, 2947, 2893, 2840, 1695, 1614, 1576, 1417, 1294, 1107, 1027, 939, 824, 768, 701. ^1H NMR (400 MHz, CDCl_3): δ 8.01 (d, $J = 8.0$ Hz, 1H), 7.81 (d, $J = 8.0$ Hz, 1H), 7.62-7.58 (m, 2H), 7.42 (td, $J = 7.6, 0.8$ Hz, 1H), 7.09 (d, $J = 12$ Hz, 1H), 6.93 (s, 1H), 4.28

(s, 1H), 4.04 (ddd, $J = 13.1, 6.0, 2.4$ Hz, 1H), 3.36 (ddd, $J = 13.1, 11.2, 4.4$ Hz, 1H), 2.94-2.85 (m, 1H), 2.74 (ddd, $J = 12.4, 4.4, 2.4$ Hz, 1H), 2.28 (s, 3H). ^{13}C NMR (100 MHz, CDCl_3): δ 167.3, 147.9, 138.4, 134.5, 133.0, 132.5, 130.4, 129.7, 129.3, 127.6, 127.3, 123.4, 123.3, 86.4, 34.7, 29.2, 21.0. HRMS-ESI (m/z) found 288.1010 and calculated 288.1000 for $\text{C}_{17}\text{H}_{15}\text{NO}_2^+$ [M+Na].

4.2.8. 12b-Hydroxy-3-bromo-5,12b-dihydro-6H-isoindolo[1,2-a]isoquinolin-8-one (CRR-228): Refluxing *N*-[2-(3-bromo-phenyl)ethyl]-phthalimide with TfOH under neat condition followed by aqueous base work up furnished the cyclized product **CRR-228** as colorless solid, 109 mg (66% yield), Mp 163 °C. IR (KBr, cm^{-1}): 3246, 2951, 2894, 2838, 1683, 1593, 1472, 1414, 1181, 1114, 1040, 939, 883, 765, 697. ^1H NMR(400 MHz, CDCl_3): δ 7.98 (d, $J = 7.5$ Hz, 1H), 7.80 (d, $J = 8.4$ Hz, 1H), 7.70-7.68 (m, 1H), 7.65 (td, $J = 7.5, 1.2$ Hz, 1H), 7.49 (td, $J = 7.5, 0.8$ Hz, 1H), 7.42 (dd, $J = 8.3, 1.8$ Hz, 1H), 7.31-7.31 (m, 1H), 4.18 (ddd, $J = 13.1, 6.1, 2.4$ Hz, 1H), 3.71 (s, 1H), 3.42 (ddd, $J = 13.1, 11.4, 4.5$ Hz, 1H), 2.99-2.91 (m, 1H), 2.80 (ddd, $J = 16.4, 4.2, 2.3$ Hz, 1H). ^{13}C NMR (100 MHz, CDCl_3): δ 167.3, 147.4, 136.9, 134.9, 132.7, 132.0, 130.3, 130.0, 129.7, 129.1, 123.5, 123.2, 122.5, 86.2, 34.4, 29.0. HRMS-ESI (m/z) found 351.9948 and calculated 351.9949 for $\text{C}_{16}\text{H}_{12}\text{BrNO}_2^+$ [M+Na].

4.2.9. 8,9-Dimethoxy-2,3,6,7-tetrahydro-1H-pyrido[2,1-a]isoquinolin-4(11bH)-one (CRR-238): Cyclization using TfOH followed by reduction using $\text{NaBH}_4/\text{MeOH}$, the *N*-[2-(2,3-dimethoxyphenyl)-ethyl]glutarimide furnished the cyclized product **CRR-238** as colorless solid, 108 mg (83% yield), Mp 95-96 °C. IR (KBr, cm^{-1}): 2952, 2833, 1693, 1493, 1464, 1417, 1331, 1276, 1223, 1080, 1046, 1003, 861, 634. ^1H NMR (400 MHz, CDCl_3): δ 6.91 (d, $J = 8.6$ Hz, 1H), 6.81 (d, $J = 8.6$ Hz, 1H), 4.84-4.80 (m, 1H), 4.60 (dd, $J = 10.4, 4.7$ Hz, 1H), 3.85 (s, 3H), 3.79 (s, 3H), 2.92-2.73 (m, 3H), 2.56-2.48 (m, 2H), 2.39-2.30 (m, 1H), 1.97-1.77 (m, 2H), 1.73-1.63 (m, 1H). ^{13}C NMR (100 MHz, CDCl_3): δ 169.4, 151.1, 146.3,

130.8, 129.8, 120.4, 110.7, 60.4, 56.5, 55.9, 39.5, 32.4, 30.7, 23.1, 19.7. HRMS-ESI (m/z) found 284.1261 and calculated 284.1263 for $C_{15}H_{19}NO_3^+$ [M+Na].

4.2.10. 12b-Hydroxy-2-hydroxy-3-methoxy-5,12b-dihydro-6H-isoindolo[1,2-a]-isoquinolin-8-one (CRR-271): Following the general procedure, *N*-[2-(3-methoxy-4-hydroxy-phenyl)ethyl]phthalimide furnished the cyclized product as colorless solid, 123 mg (83% yield), IR (KBr, cm^{-1}): 3294, 2935, 2845, 1653, 1606, 1524, 1426, 1367, 1201, 1108, 1031, 761, 682. 1H NMR (400 MHz, $CDCl_3$): δ 8.96 (s, 1H), 7.97 (d, $J = 7.6$ Hz, 1H), 7.68 (t, $J = 7.6$ Hz, 1H), 7.64 (d, $J = 7.4$ Hz, 1H), 7.51 (t, $J = 7.4$ Hz, 1H), 7.34 (s, 1H), 6.85 (s, 1H), 6.66 (s, 1H), 4.21-4.17 (m, 1H), 3.71 (s, 3H), 3.42-3.35 (m, 1H), 2.77-2.67 (m, 2H). ^{13}C NMR (100 MHz, $CDCl_3$): δ 165.8, 148.8, 147.5, 144.9, 132.2, 130.3, 129.3, 129.1, 125.0, 123.5, 122.4, 114.5, 111.8, 85.3, 55.5, 34.5, 28.3.

4.2.11. Synthesis of isoquinolinone derivative, CRR-267

(i) The imide **13** required to synthesize **CRR-267** was prepared based on the following procedure: 3,4-Dimethoxyphenethylamine **11** (250 mg, 1.4 mmol) and anhydride **12** (381 mg, 1.4 mmol) were taken in a round bottom flask containing toluene (25 mL) the mixture was refluxed at 110 °C. After 12 h the solvent was evaporated and the mixture was purified through silica gel column chromatography with hexane and ethyl acetate (1:4) mixture as eluent to furnish the imide **13** as colorless solid, 490 mg, 81% yield. FT-IR (KBr, cm^{-1}): 3067, 3001, 2942, 2831, 1769, 1700, 1030. 1H -NMR (400 MHz, $CDCl_3$): δ 7.38 (dd, $J = 3.2, 2.0$ Hz, 2H), 7.30 (dd, $J = 3.2, 2.0$ Hz, 2H), 7.16 (dd, $J = 3.2, 2.4$ Hz, 2H), 7.11 (dd, $J = 3.2, 2.4$ Hz, 2H), 6.73 (d, $J = 8$ Hz, 1H), 6.63-6.59 (m, 2H), 4.80 (s, 2H), 3.83 (s, 3H), 3.80 (s, 3H), 3.24 (m, 2H), 3.17 (s, 2H), 1.87 (m, 2H). ^{13}C -NMR (100 MHz, $CDCl_3$): δ 176.65, 148.90, 147.69, 141.44, 138.72, 130.34, 126.98, 126.74, 125.04, 124.26, 120.65, 111.80, 111.27, 55.88, 55.86, 46.79, 45.64, 39.72, 32.53.

(ii) **Cyclization of 13 to CRR-267:** An oven dried two neck round bottom flask bearing septum in side arm was cooled to room temperature under a steady stream of nitrogen gas flow. The flask was charged with stirring bar, substrate (100 mg, 0.23 mmol) and dry dichloromethane (10 mL) and cooled down to 0 °C (using ice). To this solution TfOH (0.2 mL, 8 equiv) was added with stirring. After 10 hours, the reaction mixture was quenched with water (10 mL) followed by NaHCO₃ (1g). The organic layer was separated and aqueous layer was extracted with dichloromethane (2 x 15 mL). The combined organic extract was washed with brine solution and dried over anhydrous Na₂SO₄. The extract was filtered and the solvent was removed under vacuum to dryness on rotary evaporator which yielded the cyclized product in 87 mg (87% yield).

CRR-267: Yield: 87 mg (87 %); M.p.: 162 °C. FT IR (KBr, cm⁻¹): 3406, 2966, 1667, 1514, 1438, 1357, 1262, 1129, 1023, 764. ¹H NMR (400 MHz, CDCl₃): δ 7.34-7.32 (m, 1H), 7.26-7.17 (m, 3H), 7.12-7.09 (m, 2H), 7.00 (td, *J* = 7.4, 0.96 Hz, 1H), 6.78 (td, *J* = 7.4, 0.96 Hz, 1H), 6.46 (s, 1H), 5.88 (d, *J* = 7.2 Hz, 1H), 4.74 (d, *J* = 3.8 Hz, 1H), 4.25 (d, *J* = 2.5, 1H), 4.08 (s, 1H), 3.93 (s, 1H), 3.72 (dd, *J* = 12.8, 4.7 Hz, 1H), 3.42 (dd, *J* = 8.4, 2.8 Hz, 1H), 3.16 (s, 1H), 3.08 (dd, *J* = 8.4, 2.6 Hz, 1H), 2.77 (td, *J* = 13.2, 2.7 Hz, 1H), 2.11 (dd, *J* = 15.5, 2.4 Hz, 1H), 1.26-1.18 (m, 1H). ¹³C NMR (100 MHz, CDCl₃): δ 172.8, 149.2, 147.9, 143.3, 142.0, 140.9, 137.7, 128.9, 126.6, 126.3, 126.1, 125.9, 125.3, 124.8, 124.5, 124.1, 123.5, 110.8, 110.6, 88.1, 77.3, 77.0, 76.7, 56.4, 56.0, 51.1, 48.6, 46.7, 45.6, 34.3, 27.9.

4.3. Chicken erythrocytes preparation

Unlike those of mammals, chick RBCs have intact but transcriptionally inactive nucleus.⁴⁹⁻⁵⁰ Chick RBCs possess intact antioxidant systems as that of a normal eukaryotic cell. Hence they are useful animal cell model for simulated oxidative damage in animal cells

and to monitor the response with treatment. They can be easily stored in PBS (phosphate buffered saline) at physiological pH 7.4 at 4°C.

Blood from healthy chicken was collected, centrifuged and the pellet was re-suspended in 40 mL of PBS. The number of cells in the stock was counted to be 5×10^6 /mL, from which working dilution of 1/10 was made such that the final cell count was 0.5×10^6 /mL and was used as working sample for all assays. Viability of the cells was checked each time before assays by preparing a wet film and observing under light microscope at 40x for normal cell and nuclear morphology.

The chick RBCs suspension in PBS were taken in separate tubes (1mL in each tube) and pre-treated with 4 concentrations (25 μ M, 50 μ M, 75 μ M & 100 μ M) of each compound (mentioned in Fig.2 & Fig.3) and exposed to 100 μ M H₂O₂ for 1 hour at 37°C. After the incubation period, the samples were divided as follows: 20 μ L of sample was taken for cell viability assay by acridine orange & ethidium bromide staining method, 80 μ L of the sample was allotted for comet assay, and the remaining was reserved for analysis of antioxidant status.

4.4. Analysis of protective properties

4.4.1. Acridine orange and ethidium bromide staining

AO is a cell permeable dye, when bound with double stranded DNA emits green fluorescence (emission 540 nm) under UV excitation. The dye, when bound to single stranded DNA emits orange fluorescence (emission 640 nm), thus marking damaged DNA. The staining mixture contains AO (1 mg/mL) and ethidium bromide (EB) (5 mg/mL) in phosphate buffered saline. AO is permeable in intact cell membrane where as EB is impermeable. The normal cells appear green and cells with different grades of DNA damage

vary in range from yellowish green to bright orange. After incubation, exactly 20 μ l of RBCs suspensions were taken on a clean glass slides and 7 μ l of staining solution was added, mixed well and a cover slip was placed. The wet mount was then observed under fluorescent microscope at 40 x magnification and the images were captured and processed with ProgresTM software. The cells with intact double stranded DNA appeared green and the cells with damaged DNA showed orange-red fluorescence.⁴⁹

4.4.2. Antioxidant status

The compound pre-treated and H₂O₂ exposed RBCs samples were centrifuged at 2500 x g for 5 min. The RBCs pellet was subjected to hypotonic lysis and centrifuged at 1200 x g for 10 minutes to remove cell debris. The supernatant was used for the analysis of biochemical parameters such as catalase, superoxide dismutase and the extent of lipid peroxidation. Catalase (EC 1.11.1.6) catalyses the breakdown of H₂O₂ to water and molecular oxygen. UV absorption of H₂O₂ can be measured at 240 nm, whose absorption decreases when degraded by the enzyme catalase.⁵¹ The SOD (superoxide dismutase) activity (EC 1.15.1.1) of the sample was determined by using Marklund and Marklund method.⁵² The activity of SOD was quantitatively measured by the amount of pyrogallol oxidized. The increase in the absorbance of pyrogallol was measured at 420 nm against blank containing tris-HCl buffer.

4.4.3. Lipid peroxidation

The extent of lipid peroxidation in the controls and the drug treated samples was quantified by the method of Ohkawa by thiobarbituric acid reaction.⁵³ The RBCs samples incubated were centrifuged to get the cell pellet. The supernatant was discarded and the RBCs cell pellet was lysed using distilled water. The lysate was mixed with 10 % TCA to

precipitate the proteins. Then, the samples were centrifuged and the supernatant was collected. Equal amount of supernatant and TBA were mixed and incubated in the boiling water bath for 15 minutes and the colour developed was measured at 535 nm. The results were expressed as nmols of malondialdehyde formed per minute per mg of protein.

4.4.5. Comet assay

Comet assay is a versatile technique, which is increasingly being used to quantitate DNA damage within cells. The slides were coated with 1 % normal melting point (NMP) agarose. The RBCs suspension was diluted with 0.5 % low melting point (LMP) agarose (1 in 100 dilution) and was layered on to the slide. The layer was covered with 1 % NMP. A coverslip was placed and the cells with agarose are allowed to set rapidly by chilling on ice. The slides were kept in lysis buffer (10 mM TrisHCl pH 10 with 100 mM EDTA, 2.5 M NaCl, detergents and 10 % DMSO) for one hour and were later neutralized with 0.4 M Tris pH 7.5. Electrophoresis (Dark room) was done at 50mA for 20min with alkaline buffer pH 13 and the slides were observed using fluorescent microscope at 40x objective after staining with EB of 10 mg/mL concentration. The comet images were captured under the microscope and processed using Tritex Comet Score freewareTM v1.5.

4.5. PARP-1 inhibition assay

Potential PARP-1 inhibitory activity of the novel isoquinolinone derivatives was assayed by employing Homogenous PARP-1 inhibition assay kit from Trevigen. (Trevigen, MD, USA). The reactions were performed in triplicates in a 96 well plate and the readings were obtained from FLX800 fluorescence microtitre plate reader (Biotek instruments inc, USA). The IC₅₀ values were deduced from NAD⁺ standard graph for RFU (Relative fluorescence units) and comparative derivation of PARP-1 inhibitory activity for various

dilutions as per the protocol in the Kit. A standard isoquinolinone 3, 4-dihydro-5-[4-(1-piperidiny)l)butoxyl]-1(2*H*)-isoquinolinone (DPQ) was used in the assay to compare its inhibitory potency with that of the compounds under study.

4.6. Docking studies

The interaction of the newly synthesized isoquinolinone derivatives with the PARP-1 catalytic fragment of chicken was analyzed using docking studies with Autodock 4.0. The structures of isoquinolinones were drafted using Chemskech and converted to PDB (Protein data bank) format using Pymol viewer. The PARP-1 sequence (PDB ID - 2PAW) in PDB text format was retrieved from PDB website. The sequence was processed by removal of water molecules and unwanted residues and by addition of missing residues using build/repair model option available in whatif server. The PDB format of the fixed sequence of PARP-1 catalytic fragment was used in the docking studies. The grid was set by specifically choosing the amino acids in the NAD⁺ binding pocket of PARP-1 catalytic fragment. A standard isoquinolinone 3,4-dihydro-5-[4-(1-piperidiny)l)butoxyl]-1(2*H*)-isoquinolinone (DPQ) was used to compare the binding efficiency of novel isoquinolinone derivatives.⁵⁴ The results of the docking were documented in Pymol viewer Binding energy values for the isoquinolinone derivatives were obtained from the RMSD (Root mean square deviation) table.

4.7. Statistical evaluation

Statistical analyses was performed using one-way analysis of variance (ANOVA) followed by Tukey's Multiple Range test. Differences were considered to be significant at ($P \leq 0.05$) against control group. Data were presented as mean \pm S.D of three independent samples (triplicate).

Acknowledgements

We duly acknowledge the funding support for the current study in the form of DST-FIST to the Department of Biochemistry and Molecular Biology, Pondicherry University, Puducherry. A. Suyavaran acknowledges the CSIR-UGC, New Delhi, India for junior research fellowship. C.R.R thanks CSIR and DST, New Delhi for financial support. J.S.K and S.M.R thanks respectively CSIR and UGC, New Delhi for SRF. We gratefully acknowledge CIF, Pondicherry University for NMR/IR data and the single crystal XRD facility (DST-FIST), Department of Chemistry, Pondicherry University for XRD data.

Supplementary Data

Supplementary data containing physical and spectral data of the isoquinolinones of all the isoquinolinone derivatives synthesized and investigated in the current study, can be found in the online version at ([http link to be provided by editor](http://link.to.be.provided.by.editor)).

References

1. Finkel, T.; Holbrook, N.J. *Nature* **2000**, *408*, 239.
2. Jones, D.P. *Am. J. Physiol. Cell. Physiol.* **2008**, *295*, C849.
3. Morgan, M.J.; Kim, Y.S.; Liu Z.G. *Cell Res.* **2008**, *18*, 343.
4. Zong, W.X.; Thompson, C.B. *Genes Dev.* **2006**, *20*, 1.
5. Kanduc, D.; Milletman, A.; Serpico, R.; Sinigaglia, E. *Int. J. Oncol.* **2002**, *22*, 165.
6. Van Wijk, S.J.; Hageman, G.J. *Free Radical Biol. Med.* **2005**, *39*, 81.
7. Langelier, M.F.; Plank, J.L.; Roy, S.; Pascal, J.M. *J. Biol. Chem.* **2011**, *286*, 10690.
8. Kim, M.Y.; Zhang, T.; Kraus, W.L. 2005. *Gene Dev.* **2005**, *19*, 1951.

9. Amé, J.C.; Rolli, V.; Schreiber, V.; Niedergang, C.; Apiou, F.; Decker, P. *J. Biol. Chem.* **1999**, *274*, 17860.
10. Chiarugi, A.; Meli, E. *Pharmacol. Exp. Ther.* **2003**, *305*, 943.
11. Ferraris, D.V. *J. Med. Chem.* **2010**, *53*, 4561.
12. Jagtap, P.; Szabó, C. *Nat. Rev. Drug Disc.* **2005**, *4*, 421.
13. Rhee, H.K.; Lim, S.Y.; Jung, M.J.; Kwon, Y.; Kim, M.H.; Park, H.Y. *Bioorg. Med. Chem.* **2009**, *17*, 7537.
14. Plummer, R.; Jones, C.; Middleton, M.; Wilson, R.; Evans, J.; Olsen, A.; Curtin, N.; Boddy, A.; McHugh, P.; Newell, D.; Harris, A.; Jhonson, P.; Steinfeldt, H.; Dewji, D.; Wang, D.; Robson, L.; Calvert, H. *Clin. Cancer Res.* **2008**, *14*, 7917.
15. Thomas, H.D.; Calabrese, C.R.; Batey, M.A.; Canan, S.; Hostomsky, Z.; Kyle, S.; Maegley, K.A.; Newell, D.R.; Skalitzky, D.; Wang, L.Z.; Webber, S.E.; Curtin, N.J. *Mol. Cancer Ther.* **2007**, *6*, 945.
16. Penning, T.D.; Zhu, G.D.; Ghandi, V.B.; Gong, J.; Liu, X.; Shi, Y.; Klinghofer, V.; Johnson, E.F.; Bontcheva-Diaz, V.; Bouska, J.J.; Osterling, D.J.; Olson, A.M.; marsh, K.C.; Luo, Y.; Giranda, V.L. *Med. Chem.* **2009**, *52*, 514.
17. Cheon, S.H.; Park, J.S.; Lee, J.Y.; Lee, Y.N.; Chung, B.H.; Choi, B.G.; Cho, W.J.; Choi, S.U.; Lee, C.O. *Arch. Pharm. Res.* **2001**, *24*, 276.
18. Radovits, T.; Seres, L.; Gero, D.; Berger, I.; Szabo, C.; Karck, M.; Szabo, G. *Exp. Gerontol.* **2007**, *42*, 676.
19. Pellicciari, R.; Camaioni, E.; Costantino, G.; Formentini, L.; Sabbatini, P.; Venturoni, F.; Eren, G.; Bellocchi, D.; Chiaruqi, A.; Moroni, F. *Chem. Med. Chem.* **2008**, *3*, 914.

20. Seo, J.W.; Srisook, E.; Son H.J.; Hwang, O.; Cha, Y.N.; Chi, D.Y. *Eur. J. Med. Chem.* **2008**, *43*, 1160.
21. Donawho, C.K.; Luo, Y.; Luo, Y.; Penning, T.D.; Bauch, J.L.; Bouska, J.J.; Bontcheva-Diaz, V.D.; Cox, B.F.; DeWeese, T.L.; Dillehay, L.E.; Ferguson, D.C.; Ghoreishi-Haack, N.S.; Grimm, D.R.; Guan, R.; Han, E.K.; Holley-shanks, R.R.; Hristoy, B.; Idler, K.B.; Jarvis, K.; Johnson, E.F.; Kleinberg, L.R.; Klinghofer, V.; Lasko, L.M.; Liu, X.; Marsh, K.C.; McGonigal, T.P.; Meulbroek, J.A.; Olson, A.M.; Palma, J.P.; Rodriguez, L.E.; Shi, Y.; Starvropoulos, J.A.; Tsurutani, A.C.; Zhu, G.D.; Rosenberg, S.H.; Giranda, V.L.; Frost, D.J. *Clin. Cancer Res.* **2007**, *13*, 2728.
22. Lin, C.H.; Lin, M.S.; Lin, Y.H.; Chen, I.M.; Lin, P.R.; Cheng, C.Y.; Tsai, M.C. *Pharmacology* **2003**, *67*, 202.
23. Valencia, E.; Freyer, A.J.; Shamma, M.; Fajardo, V. *Tetrahedron Lett.* **1984**, *25*, 599.
24. Alonso, R.; Castedo, L.; Dominguez, D. *Tetrahedron Lett.* **1985**, *26*, 2925.
25. Zhang, Q.; Tu, G.; Zhao, Y.; Cheng, T. *Tetrahedron* **2002**, *58*, 6795.
26. Sondhi, S.M.; Singh, N.; Johar, M.; Kumar, A. *Bioorg. Med. Chem.* **2005**, *13*, 6158.
27. Huang, Q.; Shen, H.M. *Autophagy* **2009**, *5*, 273.
28. Driessens, N.; Versteijhe, S.; Ghaddhab, C.; Burniat, A.; De Deken X.; Van Sande, J.; Dumont J.E.; Miot, F.; Corvilain, B. *Endocr. Relat. Cancer.* **2009**, *16*, 845.
29. Ghirlando, R.; Giles, K.; Gowher, H.; Xiao, T.; Xu, Z.; Yao, H.; Felsenfeld, G. *Biochim. Biophys. Acta.* **2012**, *1819*, 644.
30. Steir, A.; Bize, P.; Schull Q.; Zoll, J.; Singh, F.; Geny, B.; Gros, F.; Royer, C.; Massemin, S.; Criscuolo, F. *Front. Zool.* **2013**, *10*, 33.
31. Aggarwal, M.; Naraharishetti, S.B.; Sarkar, S.N.; Rao, G.S.; Degen, G.H.; Malik, J.K. *Arch. Environ. Contam. Toxicol.* **2009**, *56*, 139.
32. Ajila, C.M.; Prasada Rao, U.J. *Food Chem. Toxicol.* **2008**, *46*, 303-9.

33. Konat, G.W. *J. Biosci.* **2003**, 28, 57.
34. Kostadinovic, M.L.; Pavkov, T.S.; Lević, D.J.; Galonja-Coghill, T.A.; Dozet, G.K.; Bojat, N.C. *Acta. Vet. Brno.* **2011**, 80, 165.
35. Tang, X.; Yang, X.; Peng, Y.; Lin, J. *Cardiovasc. Drugs Ther.* **2009**, 23, 439.
36. (a) Selvakumar, J.; Ramanathan, C.R. *Org Biomol Chem.* **2011**, 9, 7643. (b) (b) Selvakumar, J.; Ramanathan, C. R. *Unpublished Results.*
37. Baskic, D.; Popovic, S.; Ristic, P.; Arsenijevic, N.N. *Cell Biol. Int.* **2006**, 30, 924.
38. Azad, M.B.; Chen, Y.; Henson, E.S.; Cizeau, J.; McMillan-Ward, E.; Israels, S.J.; Gibson, S.B. *Autophagy* **2008**, 4, 195.
39. Ho, K.; Yazan, L.S.; Ismail, N.; Ismail, M. *Cancer Epidemiol.* **2009**, 33, 155.
40. Yen, G.C.; Chiang, H.C.; Wu, C.H.; Yeh, C.T. *Food. Chem. Toxicol.* **2003**, 41, 1561.
41. Hsieh, T.J.; Liu, T.Z.; Chia, Y.C.; Chern, C.L.; Lu, F.J.; Chuang, M.C.; Mau, S.Y.; Chen, S.H.; Syu, Y.H.; Chen, C.H. *Food Chem. Toxicol.* **2004**, 42, 843.
42. Yumita, N.; Iwase, Y.; Watanabe, T.; Nishi, K.; Kuwahara, H.; Shigeyama, M.; Sadamoto, K.; Ikeda, T.; Umemura, S. *Anticancer Res.* **2014**, 24, 6481.
43. Karakukcu, C.; Ustidal, M.; Oztruk, A.; Baskol, G.; Saraymen, R. *Mutat. Res.* **2009**, 680, 12.
44. Li, Z.; Jiao, X.; Wang, C.; Shirley, L.A.; Elsaleh, H.; Dahl, O.; Wang, M.; Soutoglou, E.; Knudsen, E.S.; Pestell, R.G. *Cancer Res.* **2010**, 70, 8802.
45. Singh, N.P.; McCoy, M.T.; Tice, R.R.; Schneider, E.L. *Exp. Cell Res.* **1988**, 175, 184.
46. Sakaue, M.; Mori, N.; Okazaki, M.; Ishii, M.; Inagaki, Y.; Lino, Y.; Miyahara, K.; Yamamoto, M.; Kumagai, T.; Hara, S.; Yamahato, M.; Arishima, K. *J. Neurosci. Res.* **2008**, 86, 3427.
47. Rani, P.; Srivastava, V.K.; Kumar A. *Eur. J. Med. Chem.* **2004**, 39, 449.

48. Fernandes, E.; Costa, D.; Toste, S.A.; Lima, J.L.; Reis, S. *Free Radic. Biol. Med.* **2004**, *37*, 1895.
49. Kransdorf, E.P.; Wang, S.Z.; Zhu, S.Z.; Langston, T.B.; Rupon, J.W.; Ginder, G.D. *Blood* **2006**, *108*, 2836.
50. Spencer, V.A.; Davie, J.R. *J. Biol. Chem.* **2001**, *276*, 34810.
51. Clairborne, A. In Catalase activity; Grenwald, R.A., Eds.; Handbook of Methods for Oxygen Radical Research. Boca Raton, Florida: CRC Press; 1985.
52. Marklund, S.; Marklund, G. *Eur. J. Biochem.* **1974**, *47*, 469.
53. Ohkawa, H.; Ohishi, N.; Yagi, K. *Anal. Biochem.* **1979**, *95*, 51.
54. Wang, G.; Huang, X.; Li, Y.; Guo, K.; Ning, P.; Zhang, Y. *PLoS One.* **2013**, *8*, e79757.

Tables

Table 1: Effect of H₂O₂, DMSO and isoquinolinone derivatives on RBCs viability by acridine orange-ethidium bromide staining.

S.No	Sample	Percentage of viability [#]
1	RBC control	94±1.52
2	H ₂ O ₂ control	41±2.08
3	DMSO control	93.6±1.52
4	CRR-222 100 µM	72±2.64
5	CRR-203 100 µM	79.3±2.05
6	CRR-211 100 µM	65.6±3.21
7	CRR-271 100 µM	93.6±1.05
8	CRR-204 100 µM	53.6±2.08
9	CRR-228 100 µM	75.3±1.52
10	CRR-227 100 µM	82.3±2.08
11	CRR-213 100 µM	68.3±2.30
12	CRR-238 100 µM	86.6±2.51
13	CRR-267 100 µM	87.3±2.08
14	CRR-224+225 100 µM	92.6±2.30

The samples represent RBCs suspended in PBS and treated with the isoquinolinone derivatives (CRR-227 to CRR-224+225), each compound at the concentration of 100 µM, followed by H₂O₂ treatment for 1 hour.

[#]Values represent the percentage of viable cells (mean±S.D) counted at three different fields (under 40 x magnification).

Table 2: Activities of some antioxidant enzymes and lipid peroxidation level in control, H₂O₂, DMSO and isoquinolinone derivatives treated RBCs.

Samples	Catalase	Superoxide dismutase	Lipid peroxidation level
RBC Control	75.34 ± 1.24	31.54 ± 1.43	12.35 ± 1.87
H ₂ O ₂ Control	15.97±2.12	11.32 ± 1.96 *	84.32 ± 12.04
DMSO Control	69.37 ± 7.74	28.43 ± 2.54	64.98 ± 2.46
CRR-222	25 23.65 ± 1.76 *	16.32±2.43 *	36.23 ± 4.76 *
	50 31.76 ± 3.32 *	19.24 ± 2.25 *	28.21 ± 1.96 *
	75 47.53 ± 2.87	23.76 ± 2.65	14.24 ± 1.87
	100 68.46 ± 5.08	27.76 ± 1.76	20.14 ± 2.64 *
CRR-203	25 26.54 ± 2.43 *	17.34 ± 3.65 *	38.46 ± 1.28 *
	50 43.65 ± 1.76 *	19.35 ± 1.32 *	29.27 ± 3.76 *
	75 48.43 ± 1.98	23.98 ± 2.23	16.54 ± 2.64
	100 64.87 ± 1.25	28.45 ± 2.08	18.32 ± 1.49
CRR-211	25 15.31 ± 0.95 *	13.19 ± 2.45 *	53.65 ± 1.25 *
	50 16.25 ± 2.54 *	15.96 ± 2.87 *	46.37 ± 2.69 *
	75 16.46 ± 1.34 *	15.54 ± 1.96 *	41.21 ± 1.54 *
	100 16.37 ± 0.36 *	18.13 ± 3.67 *	48.32 ± 1.76 *
CRR-271	25 29.52±3.09	18.616±2.49*	52.71±3.45*
	50 51.49±3.40*	21.63±1.82*	47.15±1.29*
	75 62.57±2.44*	28.863±6.20*	26.35±3.66
	100 70.66±1.87*	30.94±2.20*	15.02±1.40
CRR-204	25 15.31 ± 0.95 *	12.65 ± 1.54 *	62.98 ± 0.32 *
	50 16.25 ± 2.54 *	11.87 ± 2.76 *	56.32 ± 1.47 *
	75 16.46 ± 1.34 *	11.48 ± 2.54 *	48.12 ± 1.34 *
	100 16.37 ± 0.36 *	11.37 ± 1.95 *	42.14 ± 1.57 *
CRR-228	25 36.597±1.58	12.8667±2.24	70.74±1.86*
	50 51.14±2.28*	14.05±3.56	54.24±2.53*
	75 56.05±3.24*	17.51±1.85*	34.52±2.07
	100 65.007±4.24*	21.58±2.65*	16.75±2.16
CRR-227	25 31.71±2.29	11.51±2.42*	53.66±1.29*
	50 50.35±1.84*	14.56±1.45*	43.76±1.94*
	75 54.56±1.78*	15.08±3.17	26.52±1.92
	100 65.35±3.32*	18.6±2.12	16.95±.62
CRR-213	25 38.65 ± 1.32 *	17.23 ± 0.76 *	28.38 ± 1.96 *
	50 46.35 ± 1.37 *	19.43 ± 2.64 *	19.12 ± 1.47 *
	75 58.28 ± 0.65	24.35 ± 1.98	16.87 ± 1.45
	100 70.43 ± 1.49	29.34 ± 1.96	16.14 ± 1.37
CRR-238	25 17.36 ± 2.35 *	11.76 ± 2.58 *	61.45 ± 2.64 *
	50 25.95 ± 3.65 *	11.48 ± 0.25 *	54.23 ± 2.76 *
	75 28.47 ± 1.54 *	11.95 ± 0.76 *	48.23 ± 2.78 *
	100 31.43 ± 1.36 *	12.98 ± 0.25 *	49.54 ± 1.46 *
CRR-267	25 46.11±2.01*	15.86±1.58	51.48±2.53*
	50 55.89±2.02*	19.63±3.23*	35.60±3.20*
	75 65.12±2.93*	23.58±1.94*	24.44±1.90
	100 67.91±5.49*	27.87±2.88*	18.10±1.67
CRR – 224+225	25 35.65±1.59	13.1033±2.24	57.145±1.98*
	50 43.84±2.11*	18.50±2.51*	46.08±3.55*
	75 53.92±2.42*	22.79±4.18*	24.70±2.61
	100 63.90±3.06*	30.52±4.64*	18.90±1.42

RBC control – RBCs suspended in PBS; DMSO control – RBCs suspended in PBS with 0.5 % DMSO; H₂O₂ control – RBCs in PBS treated with 100 μM H₂O₂;

Values represents mean ± SD, * $P \leq 0.005$ against the RBC control group, where n=3. The values are expressed as: Catalase: nmol of H₂O₂ utilized/min/mg of protein at 37°C; SOD: μmol of pyrogallol oxidized/min/mg of protein at 37°C; LPO: nmol malondialdehyde formed/ mg protein at 37°C.

Table 3 Effect of isoquinolinone derivatives on genomic DNA damage by comet assay

S.No	Sample	%DNA in Head	%DNA in tail
1	RBC control	98.32 ± 1.35	1.43 ± 0.14
2	DMSO control	99.24 ± 0.93	1.05 ± 0.25
3	H ₂ O ₂ control	52.23 ± 3.98 *	45.78 ± 3.24*
4	CRR-222 100 µM	90.45 ± 1.25	8.55 ± 0.23
5	CRR-203 100 µM	65.56 ± 2.34	34.44 ± 1.87
6	CRR-211 100 µM	56.64 ± 1.41*	42.97 ± 0.23*
7	CRR-271 100 µM	92.3±1.57	7.34±2.46
8	CRR-204 100 µM	57.29 ± 1.28*	41.96 ± 3.87*
9	CRR-228 100 µM	94.32 ± 1.25	4.55 ± 0.23
10	CRR-227 100 µM	87.56 ± 2.34	11.44 ± 1.87
11	CRR-213 100 µM	54.2 ± 5.32*	45.80 ± 4.23*
12	CRR-238 100 µM	73.84 ± 1.33	9.75 ± 1.87*
14	CRR-267 100 µM	82.45 ± 1.25	16.55 ± 0.23
15	CRR-224+CRR-225 100 µM	92.34 ± 2.34	7.43 ± 1.87

#Values represent mean ± SD, statistically evaluated by one way ANOVA followed by Tukey's test, * $P \leq 0.05$ against RBCs control group; Units were expressed as percentage of DNA in the comet head and tail (Mean ± S.D) as determined by TriTek Comet score v1.5 – software.

Table 4: Binding energy and IC₅₀ value of novel isoquinolinone derivatives for PARP-1.

Isoquinolinone derivative	Binding energy (kcal/mol)#	IC50 values for PARP-1 inhibition (nM)*
CRR-222	-6.57	1279.7±119.3
CRR-203	-7.36	865.3±130.8
CRR-211	-6.9	983.4±102.6
CRR-271	-7.88	216.2±78.2
CRR-204	-7.21	1075.6±124.3
CRR-228	-8.43	138.5±21.1
CRR-227	-7.33	976.5±127.12
CRR-213	-6.93	1371.4±113.2
CRR238	-7.36	564.8±92.2
CRR-267	-8.97	1634.7±127.5
CRR-224+CRR-225	-8.43	186.5±32.3
DPQ	-8.67	53.2±6.34

#Represents binding energies of the isoquinolinone derivatives with active site of PAPR-1.

*Represents IC₅₀ values of isoquinolinone derivatives for PARP-1 inhibition by PARP-1 fluorescence plate assay. The standard drug 3,4-dihydro-5-[4-(1-piperidinyl)butoxy]-1(2*H*)-isoquinolinone (DPQ) which is a potent inhibitor of PARP-1 is used as standard control for comparison.

Figures

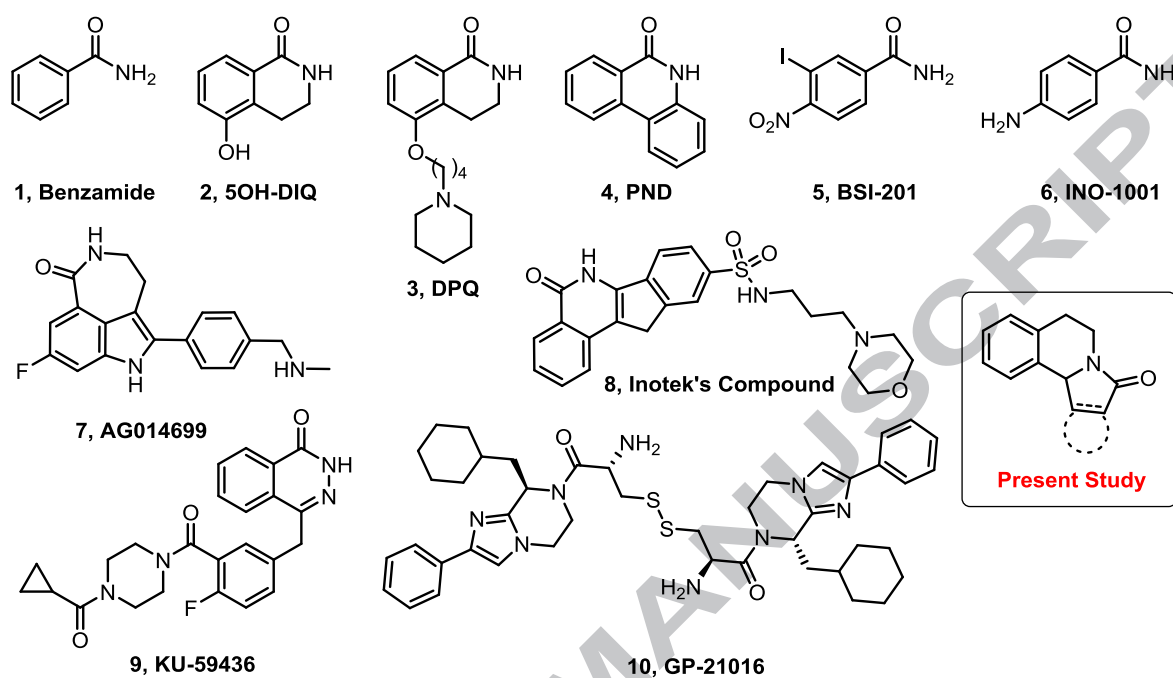


Figure 1: Structure of PARP-1 inhibitors currently in clinical trial and parent skeleton molecule used to synthesis fused isoquinolinones derivatives.

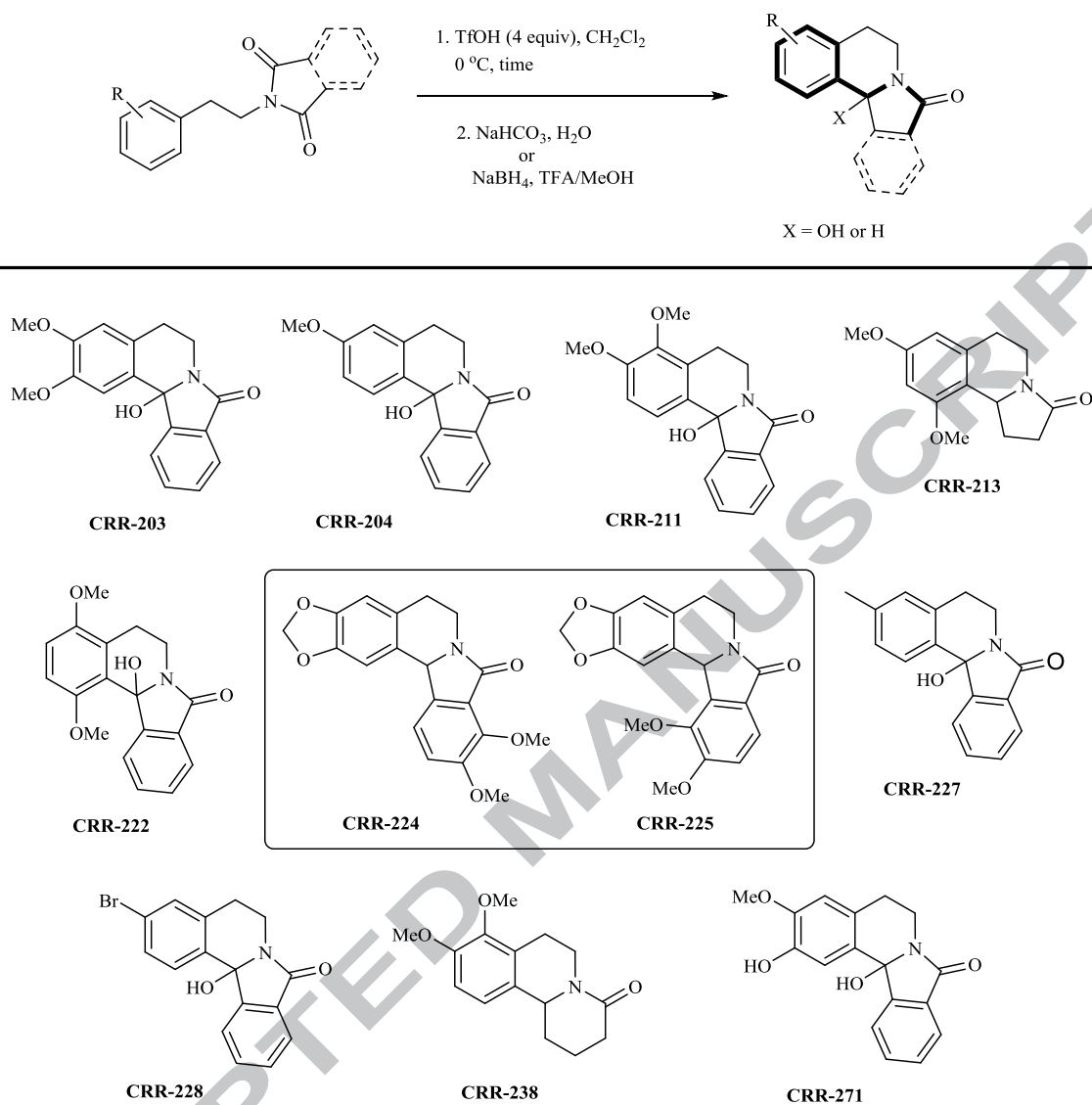


Figure 2: Structures of fused isoquinolinones derivatives synthesized and used for present investigation.

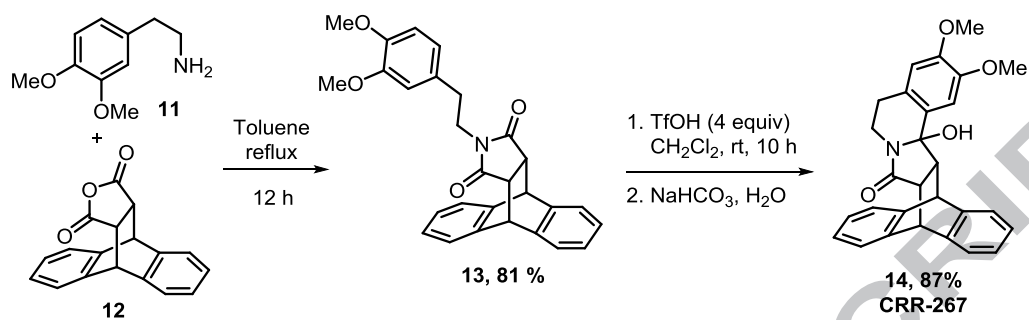


Figure 3: Scheme for synthesis of **CRR-267**.

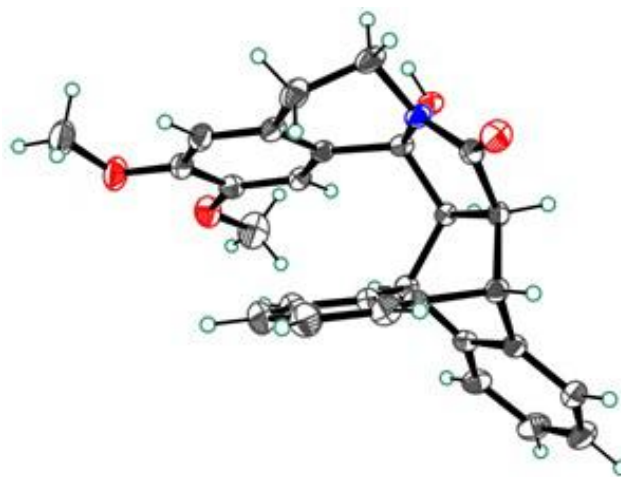


Figure 4: The crystal structure of the cyclized compound **CRR-267**.

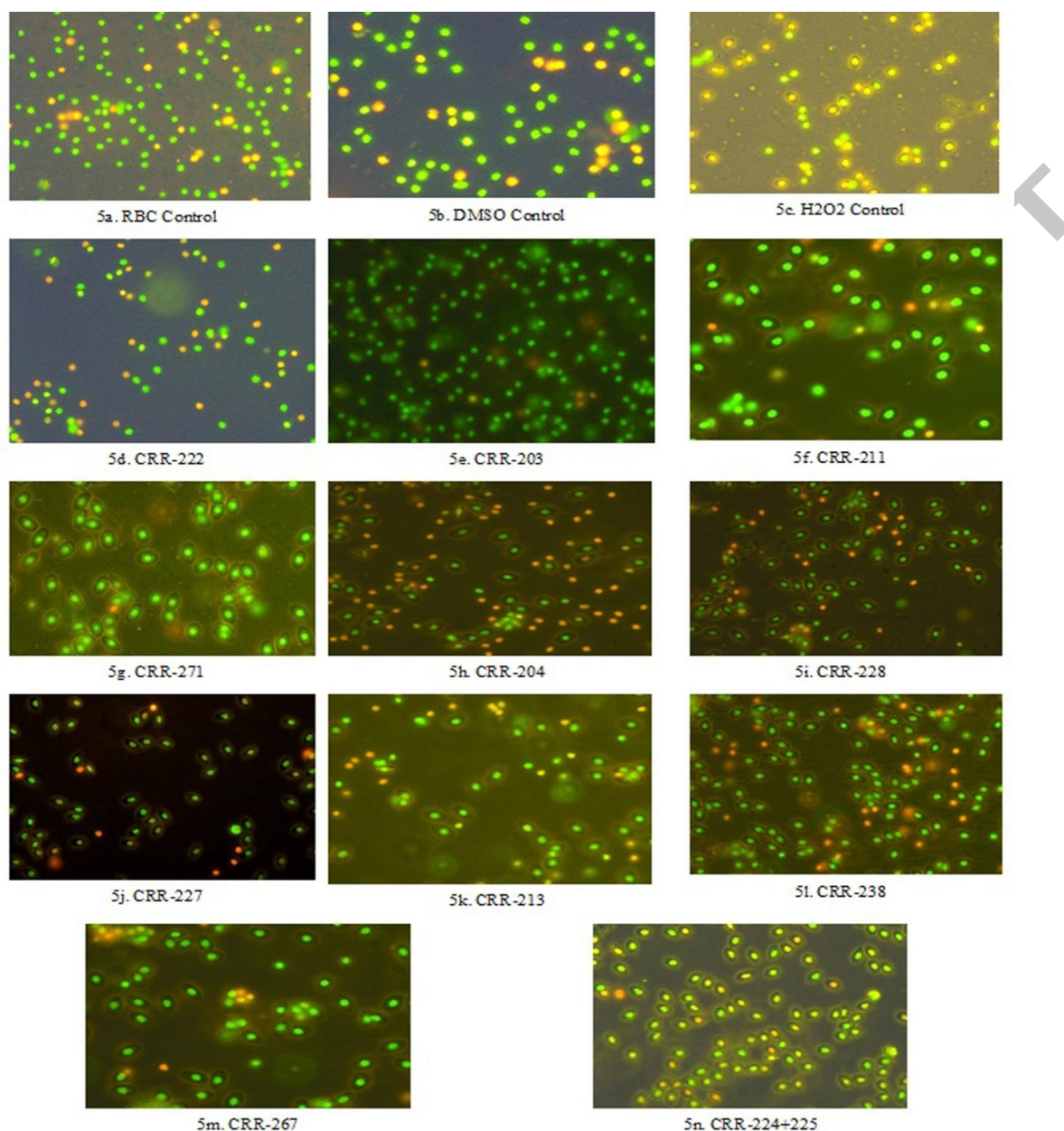


Figure 5: Shows the acridine orange & ethidium bromide staining in control and differential experimental RBCs. Fig. 5a- RBCs control (RBCs suspended in PBS); Fig. 5b - DMSO control (RBCs suspended in PBS with 0.5 % DMSO); Fig. 5c- H₂O₂ control (RBCs in PBS treated with 100 μM H₂O₂ alone); Fig. 5d to Fig. 5n - RBC treated with **CRR-222** to **CRR-224+225** (RBCs + isoquinolinone derivatives at the concentration of 100 μM + exposed to 100 μM of H₂O₂ for 1 hour at 37 °C). Images were obtained at 40 x magnification using OlympusTM CX40 fluorescence microscope.

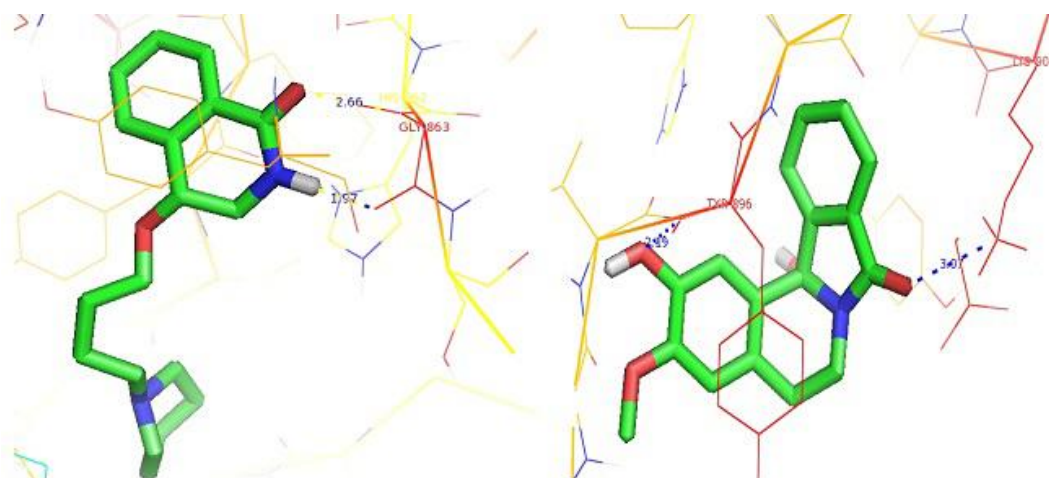


Fig 6a. DPQ with PARP1

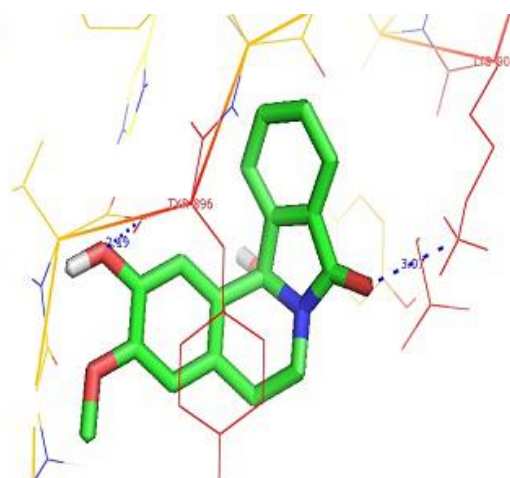


Fig 6b. CRR271 with PARP1

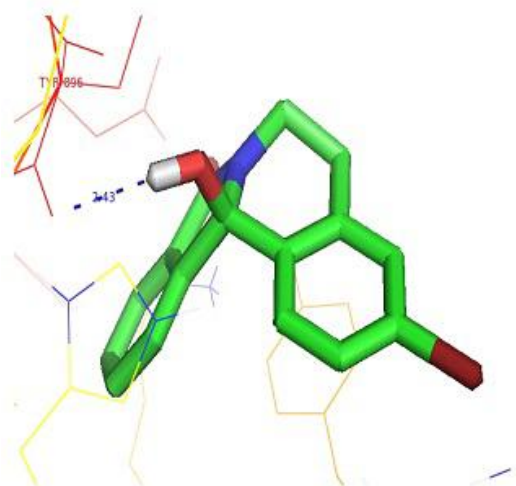


Fig 6c. CRR228 with PARP1

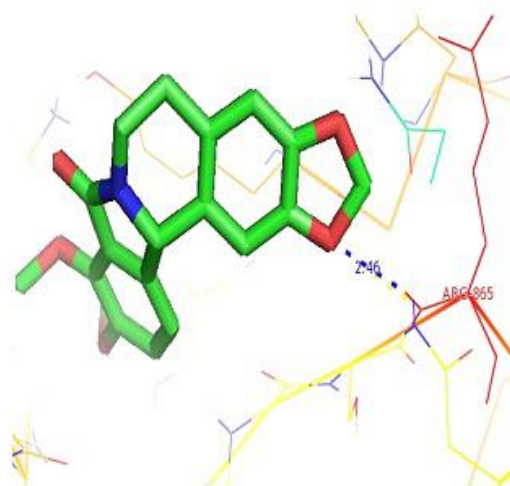


Fig 6d. CRR224+225 with PARP1

Figure 6 Molecular docking of novel isoquinolinones with PARP-1. **Fig. 6a** – DPQ forms hydrogen bond with Gly863 of PARP-1 active site; **Fig. 6b** – CRR-271 forms hydrogen bonds with Lys903, Tyr907 and Tyr896; **Fig. 6c** – CRR-228 forms hydrogen bond with Tyr896 & **Fig. 6d** – CRR-224+225 forms hydrogen bond with Gly863.

Graphical abstract

Synthesis and biological evaluation of isoindoloisoquinolinone, pyroloisoquinolinone and benzoquinazolinone derivatives as PolyADP-Ribose Polymerase-1 inhibitors

Arumugam Suyavaran^a, Chitteiti Ramamurthy^a, Ramachandran Mareeswaran^a, Yagna Viswa Shanthi^a, Jayaraman Selvakumar^b, Selvaraj Mangalaraj^b, Muthuvel Suresh Kumar^c, Chinnasamy Thirunavukkarasu^{a*} and Chinnasamy Ramaraj Ramanathan^{b*}

* Corresponding authors: E-mail address: tchinnasamy@hotmail.com; crnrath.che@pondiuni.edu.in (C. R. Ramanathan).

